NANO LETTERS

2007
Vol. 7, No. 12
3608−3611

Graphene Nanostrip Digital Memory Device

Daniel Gunlycke,*,† Denis A. Areshkin,‡ Junwen Li,§ John W. Mintmire,§ and Carter T. White*,†

Naval Research Laboratory, Washington, District of Columbia 20375, George Washington University, Washington, District of Columbia 20052, and Oklahoma State University, Stillwater, Oklahoma 74078

Received July 23, 2007; Revised Manuscript Received September 18, 2007

ABSTRACT

In equilibrium, graphene nanostrips, with hydrogens sp²-bonded to carbons along their zigzag edges, are expected to exhibit a spin-polarized ground state. However, in the presence of a ballistic current, we find that there exists a voltage range over which both spin-polarized and spin-unpolarized nanostrip states are stable. These states can represent a bit in a binary memory device that could be switched through the applied bias and read by measuring the current through the nanostrip.

Graphene has attracted much attention since it was experimentally demonstrated that the material is stable at ambient conditions.[1,2] A good portion of this attention has been focused on graphene nanostrips[3] because of their potential for device applications such as field-effect transistors[4−9] and quantum dots.[10] It has also been predicted that zigzag-edge nanostrips, such as depicted in Figure 1a, which have hydrogen atoms sp²-bonded to carbon atoms along their zigzag edges, become half metallic in the presence of a transverse electric field,[11] leading to possible spintronics[12] applications. In addition, density functional calculations have predicted that these zigzag-edge graphene nanostrips, in equilibrium, exhibit spin-polarized edge states.[13,14] In what follows, we show that this spin polarization could be eliminated by passing a ballistic current through the nanostrip, provided the applied bias voltage exceeds a given threshold. Removing the voltage causes the system to return to the spin-polarized state. We find, however, that there exists a voltage range over which both the spin-polarized and unpolarized states are stable. These two states could represent a bit in a binary memory device that can be switched through the applied bias and read by measuring the current through the nanostrip. We also find that the device should be robust at room temperature. Bias voltage has been used as a driving parameter in other recently described memory devices.[15,16]

Much of the electronic and transport properties of materials based on graphene can be understood starting from a one-parameter, nearest-neighbor, tight-binding model.[17] Although successful in describing closely related carbon nanotubes,[18,19] this model does not incorporate the essential ingredients necessary to reproduce the spin polarization in zigzag-edge graphene nanostrips found in first-principles local-density functional (LDF) calculations. We have shown, however, that this behavior can be reproduced by adding a spin-dependent scalar field ξ to the model, where $U\xi_{m,\tau}$ describes the potential experienced by an electron at site m with spin τ. The resulting one-electron Hamiltonian is given by

$$H = \gamma \sum_{\langle i,j\rangle\sigma} c_{i\sigma}^{\dagger} c_{j\sigma} + U \sum_{i\sigma} \xi_{i,\sigma} n_{i\sigma} \tag{1}$$

where $c_{i\sigma}^{\dagger}$, $c_{i\sigma}$, and $n_{i\sigma} \equiv c_{i\sigma}^{\dagger} c_{i\sigma}$ are creation, annihilation, and number operators, respectively, $\langle i,j\rangle$ denotes the set of all nearest neighbors, $\gamma \approx -2.6$ eV is the effective nearest-neighbor π-orbital hopping integral,[20,21] and U describes the strength of the spin-dependent field. The quantities $\xi_{m,\tau}$ are not adjusted to fit the first-principles results but rather determined by requiring that the free energy of the model is stationary with respect to their variations which implies that

$$\xi_{m,-\tau} = \langle n_v \rangle_{m,\tau} \tag{2}$$

where

$$\langle n_v \rangle_{m,\tau} = \int_{-\infty}^{\infty} h(E) g_v^{m\tau}(E)\, \mathrm{d}E \tag{3}$$

In eq 3, $h(E) = f(E - \epsilon_F)$, where $f(E)$ is the Fermi function with ϵ_F the Fermi level of the nanostrip, and $g_v^{m\tau}(E)$ is the local spin density of states. Because the latter depends on

* Corresponding authors. E-mail: daniel.gunlycke@nrl.navy.mil; carter.white@nrl.navy.mil.
† Naval Research Laboratory.
‡ George Washington University.
§ Oklahoma State University.

10.1021/nl0717917 CCC: $37.00
Published on Web 11/16/2007

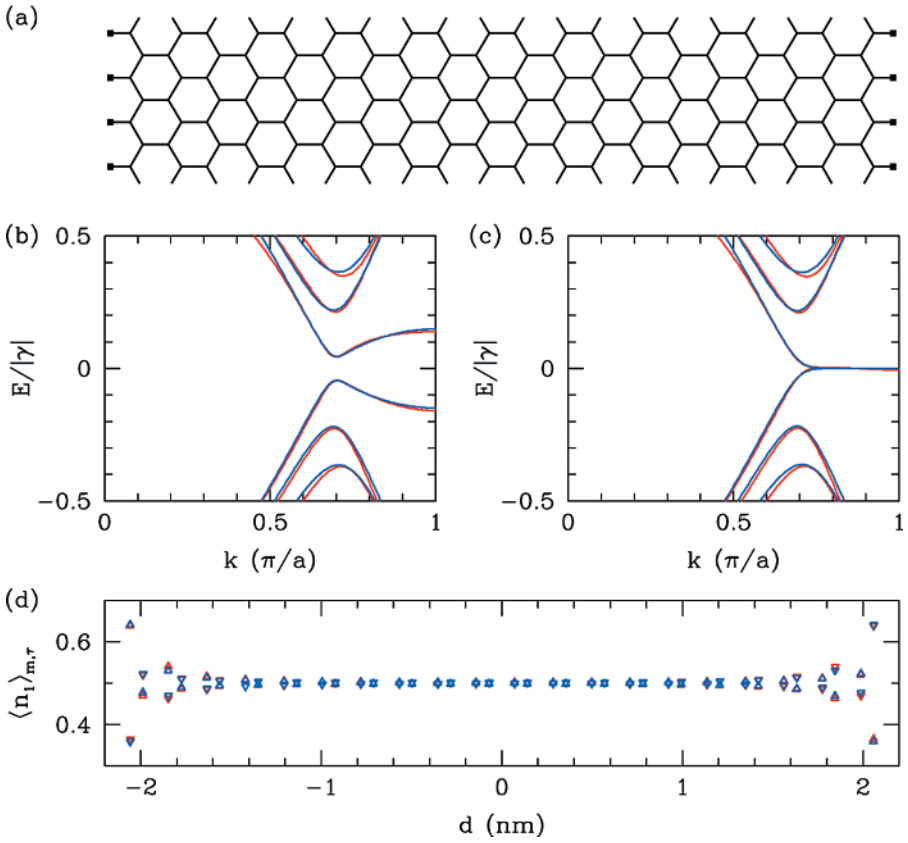

Figure 1. Geometry and self-consistent solutions for a 4.3 nm-wide zigzag-edge graphene nanostrip with carbon atoms sp^2-bonded to hydrogen atoms along its zigzag edges. (a) A transverse segment of the nanostrip with its longitudinal axis extending in the vertical direction. The nanostrip contains 40 carbon and 2 hydrogen atoms per unit cell. (b) The spin-polarized ground state energy dispersion obtained from LDF calculations (red) using an uncontracted Gaussian basis set, 7s3p and 3s for carbon and hydrogen, respectively, compared to the two-parameter model results (blue). (c) Same energy dispersions as in (b) but for the spin-restricted case. Although stationary, the unpolarized solution is unstable at zero temperature. In both (b) and (c) the Fermi level ϵ_F has been chosen to be zero. (d) Spin populations at the carbon sites from the LDF calculations (red) and the two-parameter model (blue) for the spin-polarized state. The spin directions are indicated by the triangles pointing up and down.

$\langle n_\nu \rangle_{m,\tau}$ through eqs 1 and 2, eq 3 must be solved self-consistently. Although motivated differently, eqs 1−3 are equivalent to those found from a Hartree−Fock approximation to the Hubbard model.[22,23]

The subscript, ν, refers to a particular solution of eq 3, where 0 and 1 represent the unpolarized and spin-polarized (ground state) solutions, respectively. By fitting the zero-temperature energy gap at the zone boundary obtained from the spin-polarized solution to the same gap obtained from our spin-unrestricted LDF calculations (implemented via an all-electron, linear-combination-of-atomic-orbitals method developed to treat one-dimensional systems[24,25]), we get $U = 2.75$ eV. Using this value of U, which is in line with earlier estimates,[14] the two-parameter model described by eqs 1−3 reproduces the LDF results well for both the spin-polarized and unpolarized solutions. In particular, the energy dispersions match, as do the self-consistent occupancies, $\langle n_1 \rangle_{m,\tau}$, as shown in Figure 1.

In view of the success of this two-parameter model in reproducing our first-principles results (which agree well with those of others[11,13,14]), we have extended it to include bias. Consider a zigzag-edge graphene nanostrip assumed to have a large length-to-width aspect ratio with its longitudinal axis extending from left to right (this strip orientation is perpendicular to that depicted in Figure 1a) and each strip end connected to a large contact. Also assume that the nanostrip supports ballistic transport[26,27] with all potential drops occurring at the nanostrip−contact interfaces oriented perpendicular to the hydrogen-bonded strip edges. In addition, to good approximation, assume that carriers exit from the narrow nanostrip into wide contacts with negligible probability of reflection at the interfaces.[28] This latter assumption ensures that right (left) moving states in the nanostrip are only occupied by states which originate from the left (right) contacts. Finally, suppose that the contacts provide infinite reservoirs of electrons which establish different electrochemical potentials, μ_L and μ_R, within the nanostrip for left- and right-moving electrons, respectively. The steady-state nanostrip electron distribution is then given by $h(E) = [f(E - \mu_L) + f(E - \mu_R)]/2$, where $f(E)$ is the Fermi function. Using this expression for $h(E)$ in eq 3 yields the self-consistent equations to be solved in the presence of a bias voltage, V_{ds}, between the contacts. In solving these equations, we suppose that the nanostrip remains charge neutral when $V_{ds} \neq 0$, which implies that $\mu_L = \epsilon_F - eV_{ds}/2$ and $\mu_R = \epsilon_F + eV_{ds}/2$, because of electron−hole symmetry between the valence and conduction bands.

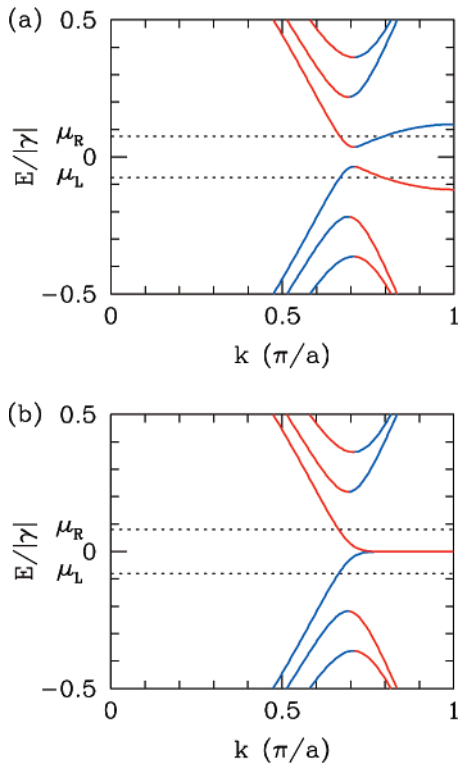

Figure 2. Loss of the spin-polarized state with increasing bias within the two-parameter model. (a) Energy dispersion of a spin-polarized graphene nanostrip with 40 carbon atoms per unit cell subject to a bias voltage 0.15 $|\gamma|/e$ at room temperature ($T = 293$ K). The application of bias voltage changes the electron occupancy in left-moving (red) and right-moving (blue) states. (b) The energy dispersion when the bias voltage has been increased to 0.16 $|\gamma|/e$. This dispersion describes the unpolarized state.

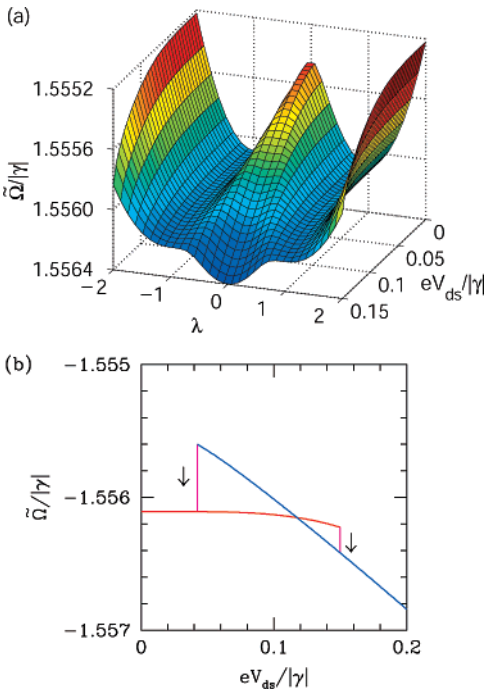

Figure 3. Stability of the spin-polarized and unpolarized states at room temperature. (a) Grand canonical potential per carbon atom, $\tilde{\Omega}$, of a zigzag-edge graphene nanostrip with 40 carbon atoms per unit cell, plotted against bias voltage, V_{ds}, and λ, where $\lambda = \pm 1$ and $\lambda = 0$ represent the spin-polarized and spin-unpolarized states, respectively. At zero bias, the unpolarized state is unstable (local maximum). When the bias voltage lies within the range $0.04 - 0.15$ $|\gamma|/e$, both states are stable. Above (Below) 0.15 $|\gamma|/e$ (0.04 $|\gamma|/e$), the spin-polarized (spin-unpolarized) state is no longer stable and the system becomes spin unpolarized (spin polarized). (b) As bias is swept, the system follows either the spin-polarized (red) or spin-unpolarized (blue) state, depending on its starting point. Because of the instabilities at the two threshold voltages (magenta), there is a hysteresis between the spin-polarized and spin-unpolarized states.

Now consider this zigzag-edge nanostrip initially in a stable spin-polarized state. As V_{ds} is increased, we find using the two-parameter model that the spin-polarized state will become unstable with respect to the unpolarized state. This instability causes the energy dispersion to change dramatically, as shown in Figure 2. The loss of stability of the spin-polarized solution can be understood by noting that, as V_{ds} is increased, some left-moving electrons, primarily in the valence band, will exit the nanostrip through the left contact without being replaced by electrons from the right contact. Simultaneously, some right-moving electrons will enter the nanostrip from the left contact and participate in the right-moving current. Once the system has reached steady state, the result can be viewed as an effective repopulation of the electronic states in the nanostrip, where electrons are "excited" from the valence band into the conduction band. Each such "excitation" depopulates a state in the valence band and populates a corresponding state with opposite spin in the conduction band. Consequently, the spin polarization is reduced, and the self-consistent conduction and valence bands move closer together. Because a narrowing gap can lead to more "excitations", positive feedback is possible. In fact, at a certain threshold bias $V_{ds}^{1\to 0}$, the spin-polarized state becomes unstable with respect to the spin-unpolarized state and the spin polarization is abruptly lost. Spin polarization in zigzag-edge nanostrips is an edge effect,[23] as evident from Figure 1d. The more localized edge states are those nearer the zone boundary in the lowest conduction and highest valence bands. At the zone boundary, the band separation is proportional to the local moment of the edge atoms, which are directly connected to hydrogen atoms; $\Delta E = |\langle n_1\rangle_{1,\uparrow} - \langle n_1\rangle_{1,\downarrow}|U \approx 0.28U$. We have found that the threshold voltage at room temperature and below can be estimated by $V_{ds}^{1\to 0} \approx 0.55\Delta E/e$. Because of the edge localization, this estimate is essentially independent of the width of the nanostrip as long as it contains more than about eight carbon atoms per unit cell.

The stability of these self-consistent solutions can be studied further by starting from a grand canonical potential[29,30] Ω, from which these solutions can be derived by requiring that $\delta\Omega/\delta\xi_{m,\tau} = 0$ for every m and τ. Treating the nanostrip as an open system, Ω is given by

$$\Omega = \Omega_\xi + \sum_\alpha (E_\alpha - TS_\alpha - \mu_\alpha N_\alpha) \qquad (4)$$

where $\Omega_\xi = -(U/2)\sum_{i\sigma} \xi_{i,\sigma}\, \xi_{i,-\sigma}$ accounts for double counting of the interaction through the field ξ and $\alpha \in \{L, R\}$ is the subsystem at temperature T with energy

$$E_\alpha = \frac{1}{2}\int_{-\infty}^{\infty} E f_\alpha(E) g(E)\, dE \quad (5)$$

electronic entropy

$$S_\alpha = -\frac{1}{2}k_B \int_{-\infty}^{\infty} \{f_\alpha(E)\ln f_\alpha(E) + [1 - f_\alpha(E)]\ln[1 - f_\alpha(E)]\}\, g(E)\, dE \quad (6)$$

and number of particles

$$N_\alpha = \frac{1}{2}\int_{-\infty}^{\infty} f_\alpha(E) g(E)\, dE \quad (7)$$

containing all left- or right-moving states. In eqs 5−7, $g(E)$ is the model total density of states of the nanostrip, k_B is Boltzmann's constant, $f_\alpha(E) = f(E - \mu_\alpha)$, and $f(E)$ is the Fermi function. Note that, in writing eqs 5−7, we have used the fact that the total density of states for either left- or right-moving states is given by $(1/2)g(E)$.

In Figure 3a, Ω, normalized per carbon atom, is plotted against V_{ds}, and λ. The latter is given by

$$\lambda = \frac{\xi_{m,-\tau} - \langle n_0\rangle_{m,\tau}}{\langle n_1\rangle_{m,\tau} - \langle n_0\rangle_{m,\tau}} \quad (8)$$

With this choice of λ, the field $\xi_{m,-\tau} = (1 - \lambda)\langle n_0\rangle_{m,\tau} + \lambda\langle n_1\rangle_{m,\tau}$ follows the shortest path between the two self-consistent solutions. Note that, $\langle n_\nu\rangle_{m,\tau} + \langle n_\nu\rangle_{m,-\tau} = 1$, because the strip is neutral, the lattice bipartite, and the dispersion relations have particle-hole symmetry. Thus, $\lambda = -1$ yields the same spin-polarized solution as $\lambda = 1$ but with all spins reversed. As can be seen in Figure 3b, the loss of the spin-polarized state at $V_{ds}^{1\to0}$ results in a decrease of Ω, which makes the process irreversible. The figure also shows the spontaneous spin polarization of the unpolarized nanostrip as the bias is reduced below a second threshold, $V_{ds}^{0\to1}$. Between the two voltages both states are stable as illustrated by Figure 3a.

The spin-polarized and unpolarized states are suitable for use in a volatile digital memory device. The device would operate at a bias voltage between $V_{ds}^{1\to0}$ and $V_{ds}^{0\to1}$. Letting V_{ds} lie outside this range would either set or clear the device. As both states are macroscopic, they are expected to be robust, even at room temperature. Any small fluctuation in the system should be quenched by the field. Consequently, we expect the memory device to be static. The hysteresis that is present in Figure 3b should also be observable in the I−V characteristics, as the spin-polarized and unpolarized states have much different low-energy transport properties. The memory information can then be read by passing a current through the device. Rather than performing a direct measurement, one could also probe a current change as voltage is swept from its operational value past one of the thresholds.

The memory device could also be implemented starting from a Peierls-distorted[31] rather than a spin-polarized system. Indeed, the hysteresis present in the I−V characteristics of some quasi-one-dimensional organic charge-transfer salts[32,33] could indicate that the necessary behavior has already been observed.

Acknowledgment. D.G., C.T.W., and J.W.M. acknowledge support from the National Academies Research Associateship Programs, the U.S. Office of Naval Research, and the U.S. Department of Energy, respectively.

References

(1) Novoselov, K. S.; Geim, A. K.; Morozov, S. V.; Jiang, D.; Zhang, Y.; Dubonos, S. V.; Grigorieva, I. V.; Firsov, A. A. *Science* **2004**, *306*, 666−669.
(2) Novoselov, K. S.; Jiang, D.; Schedin, F.; Booth, T. J.; Khotkevich, V. V.; Morozov, S. V.; Geim, A. K. *Proc. Natl. Acad. Sci.* **2005**, *102*, 10451−10453.
(3) Berger, C.; Song, Z.; Li, X.; Wu, X.; Brown, N.; Naud, C.; Mayou, D.; Li, T.; Hass, J.; Marchenkov, A. N.; Conrad, E. H.; First, P. N.; de Heer, W. A. *Science* **2006**, *312*, 1191−1195.
(4) Obradovic, B.; Kotlyar, R.; Heinz, F.; Matagne, P.; Rakshit, T.; Giles, M. D.; Stettler, M. A.; Nikonov, D. E. *Appl. Phys. Lett.* **2006**, *88*, 142102.
(5) Ouyang, Y.; Yoon, Y.; Fodor, J. K.; Guo, J. *Appl. Phys. Lett.* **2006**, *89*, 203107.
(6) Liang, G.; Neophytou, N.; Nikonov, D. E.; Lundstrom, M. S. *IEEE Trans. Electron Devices* **2007**, *54*, 677−682.
(7) Gunlycke, D.; Areshkin, D. A.; White, C. T. *Appl. Phys. Lett.* **2007**, *90*, 142104.
(8) Han, M. Y.; Özyilmaz, B.; Zhang, Y.; Kim, P. *Phys. Rev. Lett.* **2007**, *98*, 206805.
(9) Chen, Z.; Lin, Y.-M.; Rooks, M. J.; Avouris, P. *Physica E* **2007**, in press; http://dx.doi.org/10.1016/j.physe.2007.06.020.
(10) Trauzettel, B.; Bulaev, D. V.; Loss, D.; Burkard, G. *Nat. Phys.* **2007**, *3*, 192−196.
(11) Son, Y.-W.; Cohen, M. L.; Louie, S. G. *Nature* **2006**, *444*, 347−349.
(12) Wolf, S. A.; Awschalom, D. D.; Buhrman, R. A.; Daughton, J. M.; von Molna, S.; Roukes, M. L.; Chtchelkanova, A. Y.; Treger, D. M. *Science* **2001**, *294*, 1488−1495.
(13) Son, Y.-W.; Cohen, M. L.; Louie, S. G. *Phys. Rev. Lett.* **2006**, *97*, 216803.
(14) Pisani, L.; Chan, J. A.; Montanari, B.; Harrison, N. M. *Phys. Rev. B* **2007**, *75*, 064418.
(15) Szot, K.; Speier, W.; Bihlmayer, G.; Waser, R. *Nat. Mat.* **2006**, *5*, 312−320.
(16) Tseng, R. J.; Tsai, C.; Ma, L.; Ouyang, J.; Ozkan, C. S.; Yang, Y. *Nature Nano.* **2006**, *1*, 72−77.
(17) Wallace, P. R. *Phys. Rev.* **1947**, *71*, 622−634.
(18) White, C. T.; Mintmire, J. W. *J. Phys. Chem. B* **2005**, *109*, 52−65.
(19) Charlier, J.-C.; Blase, X.; Roche, S. *Rev. Mod. Phys.* **2007**, *79*, 677−732.
(20) Lomer, W. H. *Proc. R. Soc. A* **1955**, *227*, 330−349.
(21) McClure, J. W. *Phys. Rev.* **1956**, *104*, 666−671.
(22) Hubbard, J. *Proc. R. Soc. A* **1963**, *276*, 238−257.
(23) Fujita, M.; Wakabayashi, K.; Nakada, K.; Kusakabe, K. *J. Phys. Soc. Jpn.* **1996**, *65*, 1920−1923.
(24) Mintmire, J. W.; White, C. T. *Phys. Rev. Lett.* **1983**, *50*, 101−105.
(25) Mintmire, J. W.; White, C. T. *Phys. Rev. B* **1983**, *28*, 3283−3290.
(26) Areshkin, D. A.; Gunlycke, D.; White, C. T. *Nano Lett.* **2007**, *7*, 204−210.
(27) Gunlycke, D.; Lawler, H. M.; White, C. T. *Phys. Rev. B* **2007**, *75*, 085418.
(28) Szafer, A.; Stone, A. D. *Phys. Rev. Lett.* **1989**, *62*, 300−303.
(29) Todorov, T. N.; Hoekstra, J.; Sutton, A. P. *Phil. Mag. B* **2000**, *80*, 421−455.
(30) Zhang, C.-H.; Burki, J.; Stafford, C. A. *Phys. Rev. B* **2005**, *71*, 235404.
(31) Peierls, R. E. *Quantum Theory of Solids*; Oxford University Press: New York, 1955; p 108.
(32) Kumai, R.; Okimoto, Y.; Tokura, Y. *Science* **1999**, *284*, 1645−1647.
(33) Matsushita, M. M.; Sugawara, T. *J. Am. Chem. Soc.* **2005**, *127*, 12450−12451.

NL0717917